Published in final edited form as:
Stroke. 2008 January ; 39(1): 198–204. doi:10.1161/STROKEAHA.107.495598.

Albumin Therapy Improves Local Vascular Dynamics in a Rat Model of Primary Microvascular Thrombosis A Two-Photon Laser-Scanning Microscopy Study

Anitha Nimmagadda, MD, **Hee-Pyoung Park, MD, PhD**, **Ricardo Prado, MD**, and **Myron D. Ginsberg, MD**
From the Cerebral Vascular Disease Research Center, Department of Neurology, University of Miami Miller School of Medicine, Miami, Fla, USA

Abstract

Background and Purpose—High-dose human albumin is robustly neuroprotective in preclinical ischemia models and is currently in phase III clinical trial for acute ischemic stroke. To explore the hypothesis that albumin's protective effect is mediated in part by salutary intravascular mechanisms, we assessed microvascular hemodynamics in a model of laser-induced cortical arteriolar thrombosis.

Methods—The cortical microcirculation of anesthetized, physiologically monitored Sprague-Dawley rats was studied in vivo via a frontoparietal cranial window (intact dura) by two-photon laser-scanning microscopy after plasma-labeling with fluorescein-dextran. Focal thrombosis was produced in 30- to 50-μm cortical arterioles by laser irradiation. Arteriolar flow velocity was measured repeatedly by line-scanning. At 30 minutes post-thrombosis, animals were treated with either human albumin, 2 g/kg, or with saline control.

Results—Baseline arteriolar flow velocity averaged 3.5 ± 1.8 mm/s and was reduced to 10% to 13% of control values by laser-induced thrombosis, which also led to focal vasodilatation (mean, 49% above baseline diameter). Saline treatment at 30 minutes post-thrombosis failed to influence arteriolar flow velocity, which remained depressed at 10% to 22% of control throughout the subsequent 60- to 90-minute observation period. By contrast, albumin treatment induced a prompt rise in median flow velocity to 38% of control by 10 minutes post-treatment, and to 61% to 67% of control by 50 to 60 minutes.

Conclusions—High-dose albumin therapy induces a prompt, sustained improvement in microvascular hemodynamics distal to a cortical arteriolar thrombosis; these data support an important intravascular component to albumin's protective effect in acute cerebral ischemia.

Keywords

albumin; flow velocity; microcirculation; rat; thrombotic stroke; two-photon microscopy

We have shown that high-dose human albumin (ALB) confers marked neurobehavioral and histological neuroprotection in rat models of focal and global cerebral ischemia as well as

Correspondence to Myron D. Ginsberg, MD, Department of Neurology (D4–5), University of Miami Miller School of Medicine, PO Box 016960, Miami, FL 33101. E-mail E-mail: mginsberg@med.miami.edu.

Disclosures
None.

traumatic brain injury. In focal ischemia produced by temporary middle cerebral artery suture-occlusion, albumin therapy reduces cortical infarct volume by over 80%[1] with a therapeutic window of 4 to 5 hours.[2] More recently, we have completed a pilot clinical trial of albumin therapy in acute ischemic stroke that demonstrated overall safety[3] and offered preliminary suggestions of efficacy.[4] We are now conducting a large randomized multicenter trial of this therapy—the ALIAS (Albumin in Acute Stroke) trial—in patients with acute ischemic stroke.[5]

We believe that the neuroprotective efficacy of albumin is attributable to its *multifunctional* properties.[2] These include not only hemodilution and oncotic effects but also its antioxidant action, binding of copper ions, fatty-acid transport, and, importantly, a variety of *intravascular* actions. The latter include salutary interactions with vascular endothelium,[6] platelet antiaggregatory effects,[7] antagonism of erythrocyte sedimentation in low-flow states,[8] reaction with nitric oxide to form a stable *S*-nitrosothiol with endothelium-derived relaxing factor-like properties,[9] and antagonism of the binding of activated neutrophils to endothelial cells in response to inflammatory stimuli.[10] In the ALIAS pilot clinical trial, subjects who received thrombolysis (IV tissue plasminogen activator) plus *high*-dose albumin were twice as likely to attain a favorable neurological outcome at 3 months than did tissue plasminogen activator–treated subjects who received lower-dose albumin.[4] This result suggests that albumin therapy might act to maintain microvascular patency and retard reocclusion after thrombolysis.

In a previous study in rats with middle cerebral artery suture-occlusion, we used laser-scanning confocal microscopy to study the superficial cortical microcirculation in relation to ischemia, reperfusion, and albumin therapy.[11] During the first 15 to 30 minutes of postischemic recirculation, we observed prominent foci of vascular stagnation within cortical venules, which were associated with thrombus-like aggregates and probable neutrophil adhesion. Albumin therapy promptly improved venular and capillary perfusion and led to partial disappearance of adherent thrombotic material, whereas saline (control) therapy failed to have an effect.[11]

The present study was designed to characterize further the microvascular actions of albumin in a model of primary cortical microvascular thrombotic injury, utilizing the powerful method of two-photon laser-scanning excitation fluorescence microscopy (TPLSM). This method possesses numerous advantages over confocal microscopy—increased depth of tissue penetration, higher image contrast, and less photo-bleaching and photodamage to tissue. In this report, we describe a marked beneficial effect of human albumin therapy in improving microvascular flow velocity distal to laser-induced cortical arteriolar thrombosis in rats.

Materials and Methods

Animal Preparation

Fourteen male Sprague-Dawley rats (weight 330 to 400 g; Charles River Laboratories; Wilmington, Mass) were studied after an overnight fast. All study protocols were approved by the Animal Care and Use Committee of the University of Miami. Animals were anesthetized with isoflurane (3.5% for induction, 1% for maintenance), 65% nitrous oxide and a balance of oxygen. They were orotracheally intubated (14-ga shielded IV catheter, BD Insyte Autoguard), immobilized with pancuronium bromide (0.6 mg/kg IV), and mechanically ventilated. A rectal probe was inserted to measure rectal temperature, which was maintained at 37.0°C with the use of a heating pad. The right femoral artery and vein were catheterized for continuous blood pressure–monitoring, periodic arterial blood gas and plasma glucose measurements, and for drug administration. Blood gases were maintained within normal limits by ventilatory adjustments.

After catheterization, the animal was placed in a stereotactic frame and the head was immobilized with ear- and tooth-bars. A linear midline scalp incision was made, and the periosteum was removed from the skull until the suture markings were clearly identified. Hemostasis was established in the soft tissues with monopolar cautery, and in the bone by Gelfoam strips. A cranial window (4×4 mm) was created over the right or left frontoparietal cortex with the use of a drill (Leutor MiniGold power unit, Japan). The anterior and posterior margins of the cranial window were delimited by the coronal suture and lambdoid suture, respectively; the medial margin was marked by the sagittal suture, and the lateral limit by the curve of the cranium from the horizontal to the vertical plane. The dura was kept intact. The animal was then transferred to the stage of the two-photon microscope, and the stereotactic frame was attached to the microscope stage. The cranial defect was filled with artificial cerebrospinal fluid, and the temperature of the cerebrospinal fluid pool was monitored. The objective lens of the microscope was surrounded by coils of PE tubing through which water at 58°C was circulated; this helped to transfer heat to the cranium throughout the duration of the experiment to stabilize cranial temperature.

Two-Photon Laser-Scanning Microscopy System

The TPLSM system used in this study consisted of 3 major components:

1. Coherent Laser Division's Chameleon Ultra system—an ultra-fast, fully automated, widely tunable, mode-locked Ti:Sapphire laser providing femtosecond pulses. The system incorporated a solid-state Verdi laser as its pump source and featured an expanded, 350-nm tuning range (690 to 1040 nm), low noise (< 0.15%) and high output-power stability, with peak power > 2 W. The Ultra's Verdi pump-laser power was 18 W. The output of the laser system was software-controlled, allowing hands-free tuning.
2. The Coherent system was interfaced to a Bio-Rad (now Zeiss) Radiance 2100 dedicated multiphoton laser-scanning system. A two-channel motorized external detector unit was fitted with 1 bi-alkali PMT and 1 multialkali PMT and included a blue/green/red filter set. The Radiance system, incorporating a z-drive assembly and motorized beam-collimation module, was controlled by LaserSharp2000 software running on a Dell Optiplex GX260 computer. Scan modes included bidirectional scanning, z-series scans, 0° to 360° scan rotation and panning, and choice of multiple regions-of-interest.
3. The microscope was an Olympus BX51 WIF upright, fixed-stage universal research microscope. The use of special stage-risers enabled this unit to have exceptionally wide working distance, permitting the stereotactically immobilized, anesthetized rat to be placed on the microscope stage. The microscope was fitted with several lenses having high numeric aperture, long working distances as required for in vivo work, and water-immersion optics. The objective mainly used in this study was an Olympus XLUMPL 20x water-immersion plan fluorite lens, with numeric aperture=0.95. The entire system rested on a TMC antivibration table with ferromagnetic stainless steel top, gimbal pistons, and pneumatic isolator.

Induction of Microvascular Thrombosis, Treatment, and Data Acquisition

The cortical microvasculature was imaged after plasma-labeling with fluorescein isothiocyanate-dextran (70 kDa; ≈0.7 mg/kg IV). A central microscopic field within the frontoparietal craniotomy was identified by TPLSM and the local vascular architecture inspected. Next, a single medium-sized cortical arteriole (subsurface depth 10 to 20 μm) was selected at 20x magnification for subsequent study and was confirmed by its typical size (30- to 50-μm diameter; Figure 1 and Figure 2) and its very rapid flow-velocity profile (Figure 3).

The selected arteriole was imaged via z-scans performed at 1-μm intervals (Figure 1). Flow velocity was determined as previously described[12] by repetitive line-scans performed along the central longitudinal axis of the selected arteriole (512×512-pixel field; spatial dimension ≈1 μm/pixel; temporal dimension, 2 ms/pixel). The linear shadows produced by nonfluorescent particles within the plasma stream permitted computation of arteriolar flow velocity, which was proportional to the slope $\Delta x/\Delta t$ (Figure 3).

To produce localized vascular injury to this arteriole, we used the method of Nishimura et al.[13] A segment of the arteriole of interest was selected at the maximal optical zoom setting for laser-irradiation at the two-photon wavelength of 800 nm. Irradiation intensity (W/cm^2) was set according to the vessel diameter. The vessel was then irradiated over a period of ≈5 minutes. Laser pulses (800-nm wavelength; energy, 264 watts) were delivered to a ≈35×70-μm rectangular target aligned along the arteriole's longitudinal axis (via the 20x microscope objective at 10x optical zoom) to induce a thrombus occupying the entire luminal cross-section. The onset of thrombosis was identified by the dilatation of the irradiated segment, the emergence of bright fluorescence along the vessel wall, and by a nonfluorescent mass within the irradiated arteriole (Figure 1). The laser pulse energy was held beneath the level needed to induce dye extravasation and vessel rupture.[13] If vascular rupture occurred, the animal was discarded from the series.

Animals with successful arteriolar thrombosis were then randomly allocated by coin toss to treatment with either 25% ALB, 2.5 g/kg (Baxter Bioscience; n = 8), or a comparable volume of isotonic saline (n = 6). This treatment (IV infusion over 3 minutes) was begun at 30 minutes after vascular injury. Microvascular flow velocity in the arteriolar segment immediately distal to thrombosis was determined in all rats by successive line-scans beginning 10 minutes before injury and at subsequent 5-minute intervals throughout the 30-minute post-thrombosis pretreatment period, and for at least 60 minutes after treatment. In 5 ALB-treated rats and 5 saline-treated rats, post-treatment scans were continued out to 90 minutes. Z-scan images of the arteriole and its injury-site were performed immediately before injury, at 30 minutes postinjury, and at the end of the 60-or 90-minute post-treatment observation period. The resultant images were subjected to close inspection during the study and were stored for later visual analysis by means of Image ProPlus software.

Results

Physiological Variables

These are shown in the Table for the pooled series; there were no differences between the ALB and saline groups for any physiological variable. In both groups, temperatures measured in the artificial cerebrospinal fluid pool superficial to the craniotomy were 34 ± 3.5°C throughout the experiment.

Microvascular Morphology

Typical cortical arterioles selected for study are shown in Figure 1 and Figure 2. They exhibited occasional branching (Figure 2). Baseline arteriolar diameter for the series was 33.2 ± 7.7 μm (mean ± SD). Successful thrombus induction was signaled by dark focal interruptions of intravascular FITC fluorescence, often rimmed by bright fluorescence accumulations in the overlying walls of the dilated arteriole (Figure 1). The diameter of the thrombosed arteriole increased to 49.5 ± 15.7 μm, or 49% above baseline. At the end of the post-treatment observation period, arteriolar diameter in the ALB group had increased by 12 ± 2% above the immediate pretreatment value; in the saline group, this increase was 9 ± 5% (*P* = not significant). In most animals, treatment with ALB or saline failed to influence the microscopic morphology of the occluded arteriole, which remained grossly unchanged throughout the post-

treatment observation period. In other instances (Figure 2), ALB treatment was associated with subtle focal morphological changes.

Arteriolar Flow-Velocity Measurements

Figure 3 illustrates line-scans used to measure arteriolar flow velocity. At baseline before induction of thrombosis, mean arteriolar flow velocity was identical in the ALB and saline groups: ALB, 3.4 ± 1.7 mm/s (mean ± SD, n = 8); saline, 3.6 ± 1.8 mm/s (n = 6). Subsequent flow-velocity measurements in each rat were normalized to that animal's baseline value. After induction of arteriolar thrombosis, median flow velocity distal to the thrombus declined precipitously (ALB group, 10.4% of control; saline group, 13.1% of control; *P* = not significant, Mann-Whitney test) and remained steady throughout the subsequent 30 minutes (Figure 4).

Saline treatment failed to influence arteriolar flow velocity, which remained constant at median values of 10% to 22% of control throughout the subsequent 60 to 90-minute observation period (Figure 4 and Figure 5). By contrast, in ALB-treated rats, median flow velocity rose to 38% of control within 10 minutes of ALB administration. By 50 to 60 minutes after ALB treatment, median flow velocity had risen to 61% to 67% of control (Figure 4 and Figure 6). The time-course of arteriolar flow-velocity measurements, together with z-scan images, are depicted for a representative saline-treated and ALB-treated rat in Figure 5 and Figure 6, respectively.

Discussion

The present study was conducted in a physiologically controlled model of laser-induced cortical arteriolar thrombosis resulting in a high-grade but nonzero decrement in flow velocity; thus, the thrombotic lesion was subocclusive. The likely mechanism of clot formation in this model is primary endothelial and basement membrane injury, which triggers the endogenous clotting cascade.[13] In this model, the administration of high-dose human albumin resulted in a prompt, sustained improvement in flow velocity distal to an arteriolar thrombus, despite an absence of consistent changes in thrombus size or morphology (Figure 2 and Figure 6). The precise mechanism underlying this phenomenon requires further study but may be attributable to an effect of ALB in reducing the spatial extent of adhesion of the thrombus to the underlying endothelium or to a microscopic loosening of the texture of the thrombus itself. Enhancement of flow in collateral branches supplying the thrombosed arteriole also needs to be considered but is unlikely inasmuch as flow velocity in our study was measured just distal to the thrombus, upstream from any possible collaterals.

The present results are consonant with the salutary intravascular action of ALB in reversing postischemic venular thrombosis observed in our previous confocal-microscopic study of middle cerebral artery suture-occlusion[11] (described in the Introduction). Furthermore, they lend support to the speculative hypothesis generated by the efficacy-analysis of our recently published ALIAS pilot clinical trial: namely, that a prominent component of albumin's protective effect is mediated within in the vascular compartment and may relate to an antithrombotic action that helps to loosen microvascular thrombi and to retard reocclusion after pharmacological thrombolysis.[4] We have demonstrated a flow-enhancing role of ALB in previous studies by means of autoradiography[14] and laser Doppler flowmetry.[11,15]

TPLSM differs from confocal microscopy in that it is a nonlinear approach that depends on the excitation of a fluorophore by 2 photons arriving within an extraordinarily narrow time window ($\approx 10^{-18}$ seconds). Two-photon fluorescence excitation is confined to a small zone within the focal plane where the photon-density is high[16,17]; and the deep red or near-infrared excitation wavelengths used in TPLSM penetrate tissue better than the visible wavelengths used in confocal microscopy.[17] Thus, the advantages of two-photon over confocal microscopy are the far greater depth of tissue penetration (up to ≈500 μm or more), greater light collection

efficiency, the confining of photobleaching and photodamage to the imaged zone, higher resolution, and higher contrast.[16,17] In addition, two-photon excitation at a single wavelength can stimulate fluorescence emission in fluorophores having a broad range of excitation maxima, permitting multiple fluorophores to be imaged simultaneously. TPLSM has been successfully applied in vivo to study tumorigenesis,[18] and the evolution of senile plaques[19] and amyloid deposition[20] in models of Alzheimer disease.

Several authors have used TPLSM to study anoxic or hypoglycemic hippocampal slice preparations (eg, dendritic reorganization,[21] synaptic spine alterations denoting plasticity,[22] hypoxic tolerance,[23] and protection conferred by microglial activation[24]). However, only 2 published studies have applied TPLSM in vivo to whole-animal studies of cerebral ischemia: Nishimura et al[13] used TPSLM to produce 3 gradations of microvascular injury: frank rupture with local hemorrhage, intravascular clot (resembling the methods of our study), and extravasation of blood components at the lowest energies. In a report from the same group,[25] TPLSM was used to study hemodynamics in penetrating cerebral arterioles that were occluded via rose-bengal photochemistry. Other workers, however, have used the related methods of intravital high-speed confocal and widefield microscopy with great success to study, in real-time, the roles of platelets, blood coagulation products, endothelium and vessel wall in the process of thrombus formation in the mouse cremaster muscle preparation.[26–28]

In summary, the present study has used two-photon microscopy to provide evidence that human albumin administration beneficially influences microvascular hemodynamics in a model of nonthrombolysed microvascular thrombosis. These results add further evidence supporting the neuroprotective potential of albumin therapy in ischemic stroke.

Acknowledgments

Sources of Funding

This study was supported by NIH grants NS05820 and NS46295.

References

1. Belayev L, Zhao W, Pattany PM, Weaver RG, Huh PW, Lin B, Busto R, Ginsberg MD. Diffusion-weighted magnetic resonance imaging confirms marked neuroprotective efficacy of albumin therapy in focal cerebral ischemia. Stroke 1998;29:2587–2599. [PubMed: 9836772]
2. Belayev L, Liu Y, Zhao W, Busto R, Ginsberg MD. Human albumin therapy of acute ischemic stroke: marked neuroprotective efficacy at moderate doses and with a broad therapeutic window. Stroke 2001;32:553–560. [PubMed: 11157196]
3. Ginsberg MD, Hill MD, Palesch YY, Ryckborst KJ, Tamariz D. The ALIAS Pilot Trial: a dose-escalation and safety study of albumin therapy for acute ischemic stroke. I. Physiological responses and safety results. Stroke 2006;37:2100–2106. [PubMed: 16809571]
4. Palesch YY, Hill MD, Ryckborst KJ, Tamariz D, Ginsberg MD. The ALIAS Pilot Trial: a dose-escalation and safety study of albumin therapy for acute ischemic stroke. II. Neurological outcome and efficacy-analysis. Stroke 2006;37:2107–2114. [PubMed: 16809570]
5. Ginsberg MD, Palesch YY, Hill MD. The ALIAS (ALbumin In Acute Stroke) Phase III randomized multicentre clinical trial: design and progress report. Biochem Soc Trans 2006;34:1323–1326. [PubMed: 17073812]
6. Schnitzer JE, Oh P. Albondin-mediated capillary permeability to albumin: differential role of receptors in endothelial transcytosis and endocytosis of native and modified albumins. J Biol Chem 1994;269:6072–6082. [PubMed: 8119952]
7. Tokumura A, Yoshida J, Maruyama T, Fukuzawa K, Tsukatani H. Plate-let aggregation induced by ether-linked phospholipids. 1. Inhibitory actions of bovine serum albumin and structural analogues of platelet activating factor. Thromb Res 1987;46:51–63. [PubMed: 3647677]

8. Reinhart WH, Nagy C. Albumin affects erythrocyte aggregation and sedimentation. Eur J Clin Invest 1995;25:523–528. [PubMed: 7556371]
9. Keaney JFJ, Simon DI, Stamler JS, Jaraki O, Scharfstein J, Vita JA, Loscalzo J. NO forms an adduct with serum albumin that has endothelium-derived relaxing factor-like properties. J Clin Invest 1993;91:1582–1589. [PubMed: 8473501]
10. Lang JD Jr, Figueroa M, Chumley P, Aslan M, Hurt J, Tarpey MM, Alvarez B, Radi R, Freeman BA. Albumin and hydroxyethyl starch modulate oxidative inflammatory injury to vascular endothelium. Anesthesiology 2004;100:51–58. [PubMed: 14695724]
11. Belayev L, Pinard E, Nallet H, Seylaz J, Liu Y, Riyamongkol P, Zhao W, Busto R, Ginsberg MD. Albumin therapy of transient focal cerebral ischemia: in vivo analysis of dynamic microvascular responses. Stroke 2002;33:1077–1084. [PubMed: 11935064]
12. Kleinfeld D, Mitra PP, Helmchen F, Denk W. Fluctuations and stimulus-induced changes in blood flow observed in individual capillaries in layers 2 through 4 of rat neocortex. Proc Natl Acad Sci U S A 1998;95:15741–15746. [PubMed: 9861040]
13. Nishimura N, Schaffer CB, Friedman B, Tsai PS, Lyden PD, Kleinfeld D. Targeted insult to subsurface cortical blood vessels using ultrashort laser pulses: three models of stroke. Nat Methods 2006;3:99–108. [PubMed: 16432519]
14. Huh PW, Belayev L, Zhao W, Busto R, Saul I, Ginsberg MD. The effect of high-dose albumin therapy on local cerebral perfusion after transient focal cerebral ischemia in rats. Brain Res 1998;804:105–113. [PubMed: 9729310]
15. Liu Y, Belayev L, Zhao W, Busto R, Belayev A, Ginsberg MD. Neuro-protective effect of treatment with human albumin in permanent focal cerebral ischemia: histopathology and cortical perfusion studies. Eur J Pharmacol 2001;428:193–201. [PubMed: 11675036]
16. Oheim M, Michael DJ, Geisbauer M, Madsen D, Chow RH. Principles of two-photon excitation fluorescence microscopy and other nonlinear imaging approaches. Adv Drug Deliv Rev 2006;58:788–808. [PubMed: 17055106]
17. Svoboda K, Yasuda R. Principles of two-photon excitation microscopy and its applications to neuroscience. Neuron 2006;50:823–839. [PubMed: 16772166]
18. Helmchen F, Denk W. Deep tissue two-photon microscopy. Nat Methods 2005;2:932–940. [PubMed: 16299478]
19. Christie RH, Bacskai BJ, Zipfel WR, Williams RM, Kajdasz ST, Webb WW, Hyman BT. Growth arrest of individual senile plaques in a model of Alzheimer's disease observed by in vivo multiphoton microscopy. J Neurosci 2001;21:858–864. [PubMed: 11157072]
20. Bacskai BJ, Hickey GA, Skoch J, Kajdasz ST, Wang Y, Huang GF, Mathis CA, Klunk WE, Hyman BT. Four-dimensional multiphoton imaging of brain entry, amyloid binding, and clearance of an amyloid-beta ligand in transgenic mice. Proc Natl Acad Sci U S A 2003;100:12462–12467. [PubMed: 14517353]
21. Piccini A, Malinow R. Transient oxygen-glucose deprivation induces rapid morphological changes in rat hippocampal dendrites. Neuropharmacology 2001;41:724–729. [PubMed: 11640926]
22. Jourdain P, Nikonenko I, Alberi S, Muller D. Remodeling of hippocampal synaptic networks by a brief anoxia-hypoglycemia. J Neurosci 2002;22:3108–3116. [PubMed: 11943814]
23. Buchner M, Huber R, Riepe MW. Trans-synaptic increase of hypoxic tolerance in hippocampus upon physical challenge with two-photon microscopy. Hippocampus 2002;12:765–773. [PubMed: 12542228]
24. Neumann J, Gunzer M, Gutzeit HO, Ullrich O, Reymann KG, Dinkel K. Microglia provide neuroprotection after ischemia. FASEB J 2006;20:714–716. [PubMed: 16473887]
25. Nishimura N, Schaffer CB, Friedman B, Lyden PD, Kleinfeld D. Penetrating arterioles are a bottleneck in the perfusion of neocortex. Proc Natl Acad Sci U S A 2007;104:365–370. [PubMed: 17190804]
26. Falati S, Gross P, Merrill-Skoloff G, Furie BC, Furie B. Real-time in vivo imaging of platelets, tissue factor and fibrin during arterial thrombus formation in the mouse. Nat Med 2002;8:1175–1181. [PubMed: 12244306]
27. Furie B, Furie BC. Thrombus formation in vivo. J Clin Invest 2005;115:3355–3362. [PubMed: 16322780]

28. Vandendries ER, Hamilton JR, Coughlin SR, Furie B, Furie BC. Par4 is required for platelet thrombus propagation but not fibrin generation in a mouse model of thrombosis. Proc Natl Acad Sci U S A 2007;104:288–292. [PubMed: 17190826]

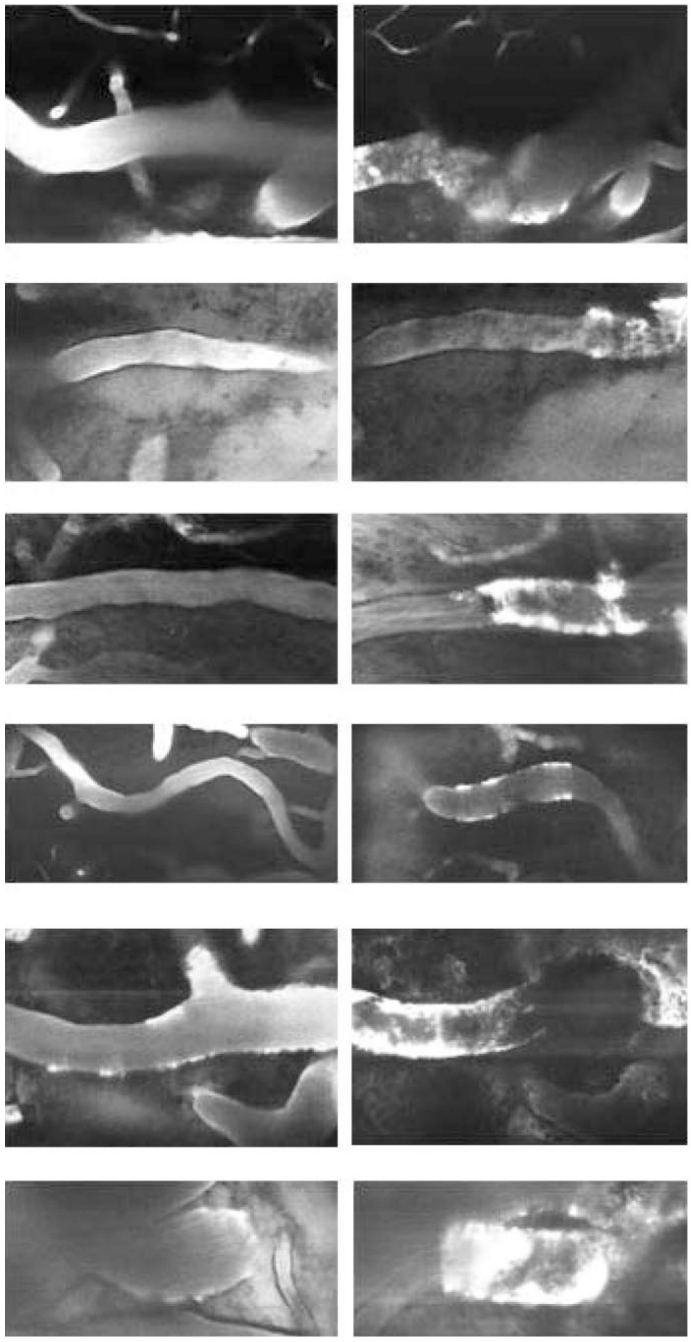

Figure 1.
Representative 30- to 50-μm cortical arterioles visualized by TPLSM after intravenous administration of FITC-dextran. Left column: appearance at baseline, before thrombosis. Right column: 30 minutes after thrombus-induction. Thrombosis is evident by irregular interruption of the dye column. The thrombosed vascular segments are variably dilated, and there is focal plasma extravasation into vessel walls, denoting vascular injury (20x objective).

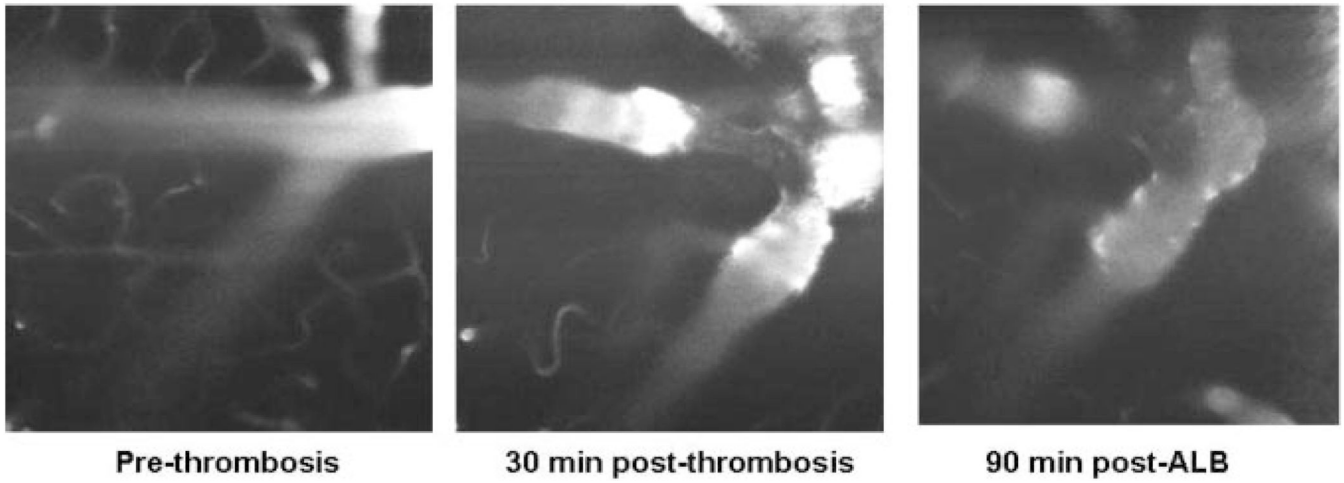

Figure 2.
Left panel: arteriolar field at baseline. Middle panel: at 30 minutes after induction of thrombosis, the thrombosed arteriolar segment is evident by an absence of FITC fluorescence, and focal narrowing is present. Right panel: 90 minutes after ALB treatment, the vasoconstriction is diminished, and the plasma column has become more regular in diameter.

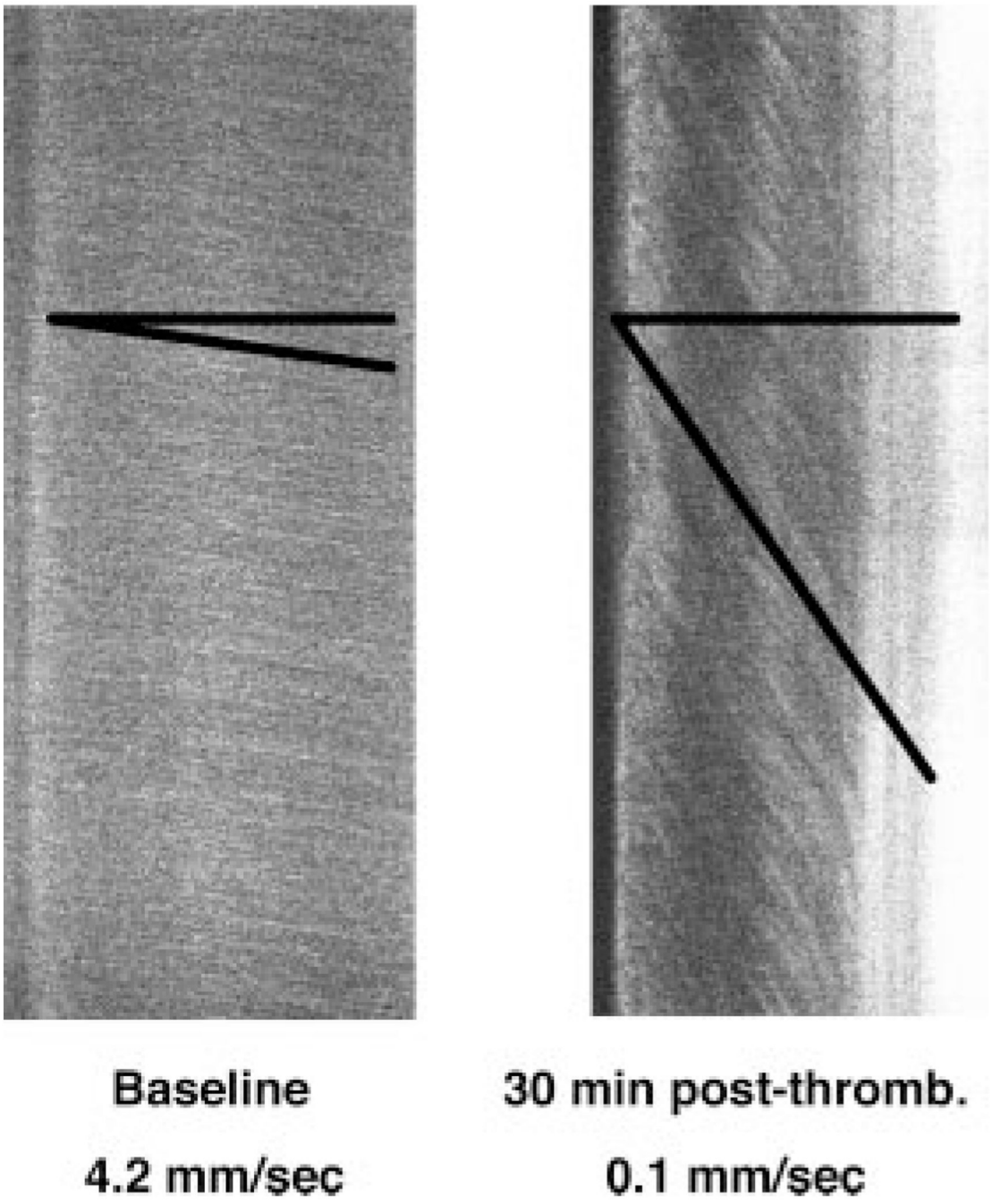

Figure 3.
Examples of line-scans used to measure microvascular flow-velocity along the longitudinal axis of arterioles of interest. Top-to-bottom sweep-duration is 1024 ms. The slopes ($\Delta x/\Delta t$) of the measurement-angles are proportional to flow velocity. Left: rapid baseline flow velocity; right, markedly reduced flow velocity distal to arteriolar thrombosis.

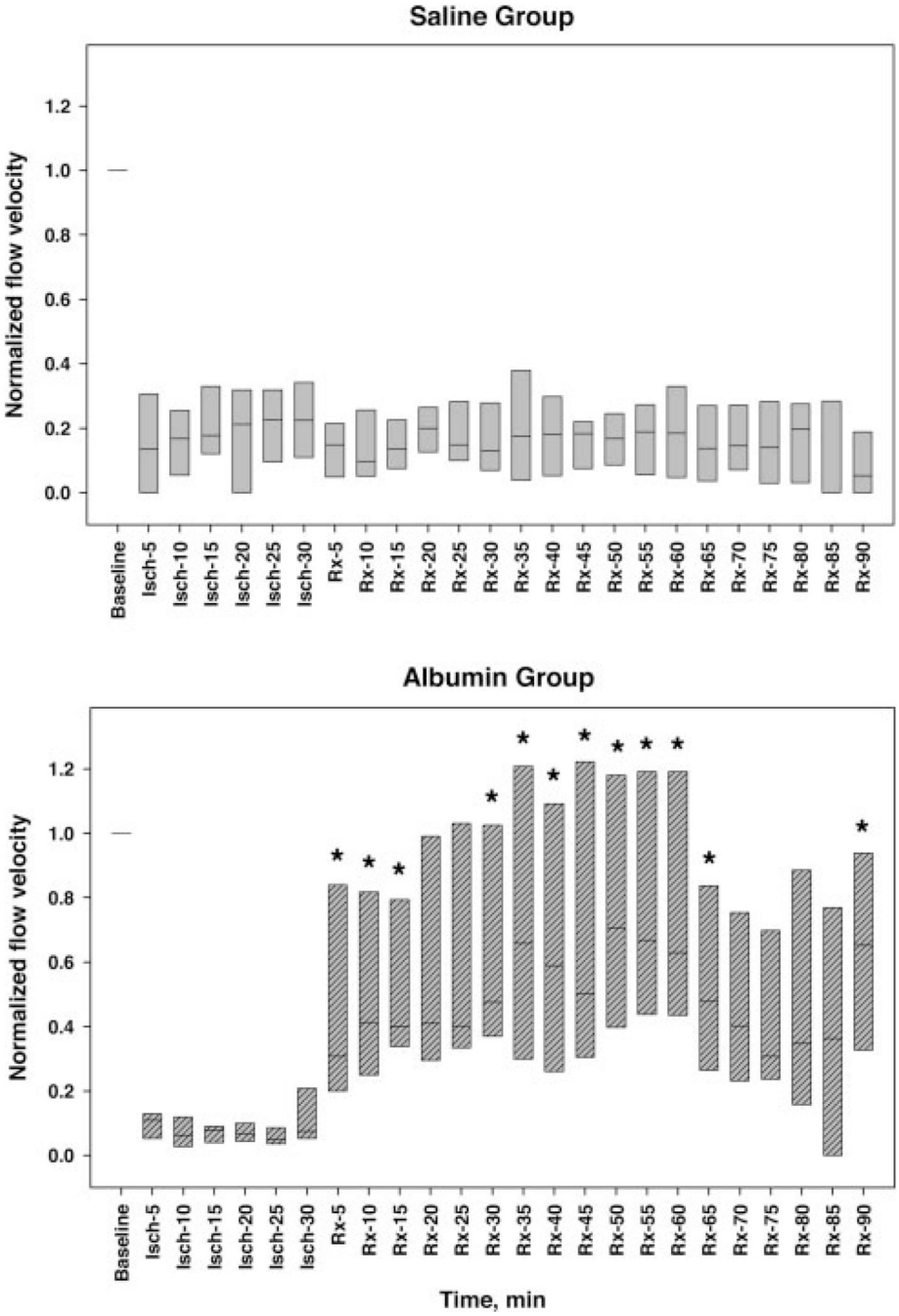

Figure 4.

Arteriolar flow velocity, normalized to each animal's baseline velocity value, measured at baseline, during 30-minute thrombosis before treatment (Isch-5 through -30), and up to 60 minutes (total n = 14) or 90 minutes (n = 10) after treatment with either isotonic saline control (upper panel) or 2.5 g/kg of 25% human albumin (Rx-5 through -90; lower panel). Bars span the 25th to 75th percentiles; lines within each bar denote median values. Thrombus-induction led to precipitous declines in median flow velocity to ≈80% to 95% below baseline values. Saline administration failed to improve arteriolar flow velocity (upper panel), whereas albumin treatment resulted in a rapid flow-velocity improvement (lower panel). (The "step" seen after 60 minutes is due to the fact that only 5 of the initial cohort of 8 ALB rats were studied between

65 and 90 minutes of treatment). *, $P<0.05$ versus corresponding saline group, Mann-Whitney rank sum test.

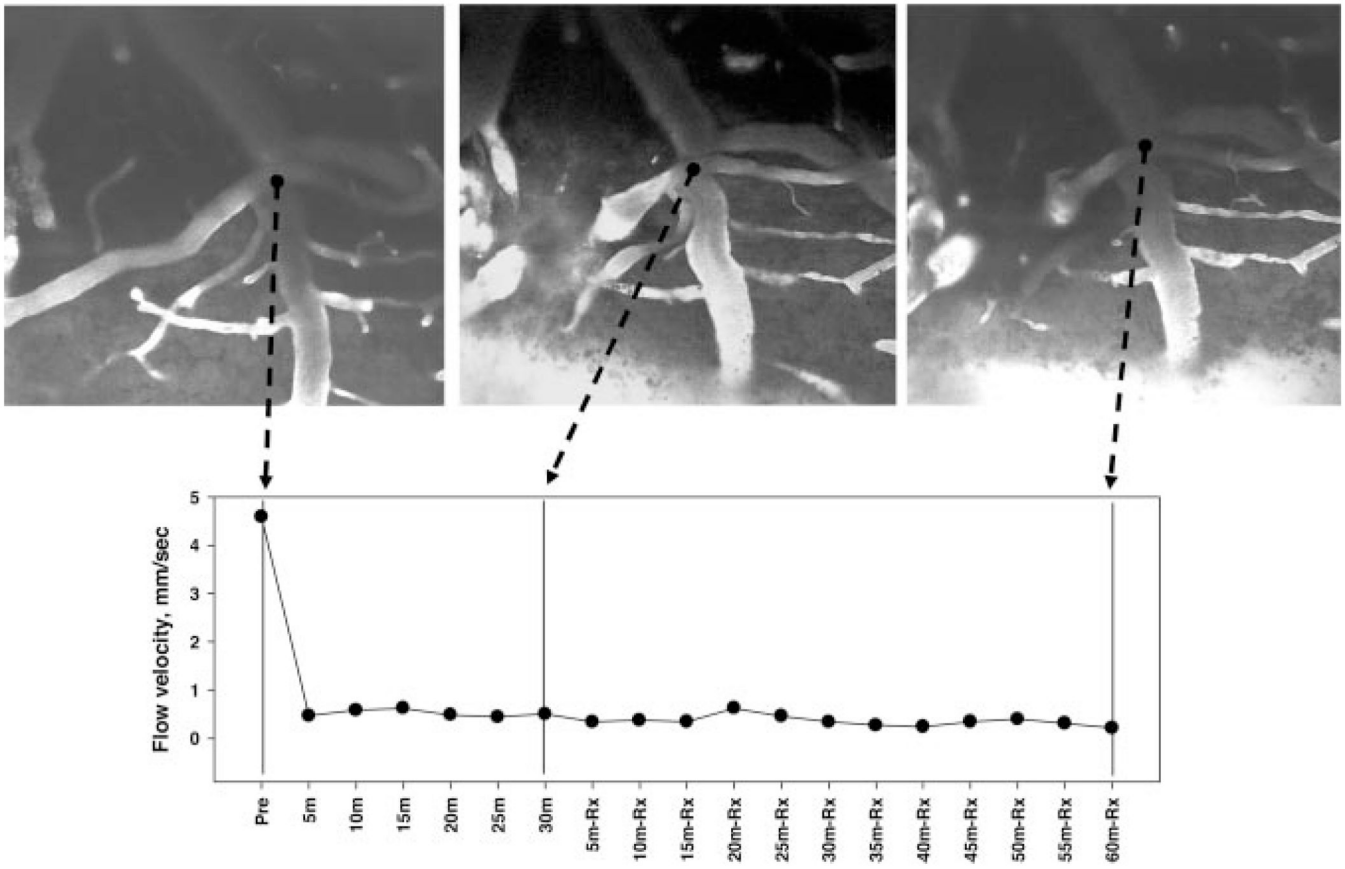

Figure 5.

Upper panels: cortical arteriole visualized with FITC-dextran at baseline (left), at 30 minutes after laser-induced thrombosis (middle), and at 90 minutes after treatment with saline control (right). Lower panel presents microvascular flow velocities measured by line-scanning at 5-minute intervals. Saline therapy failed to affect microvascular perfusion velocity distal to arteriolar thrombosis. (20x objective).

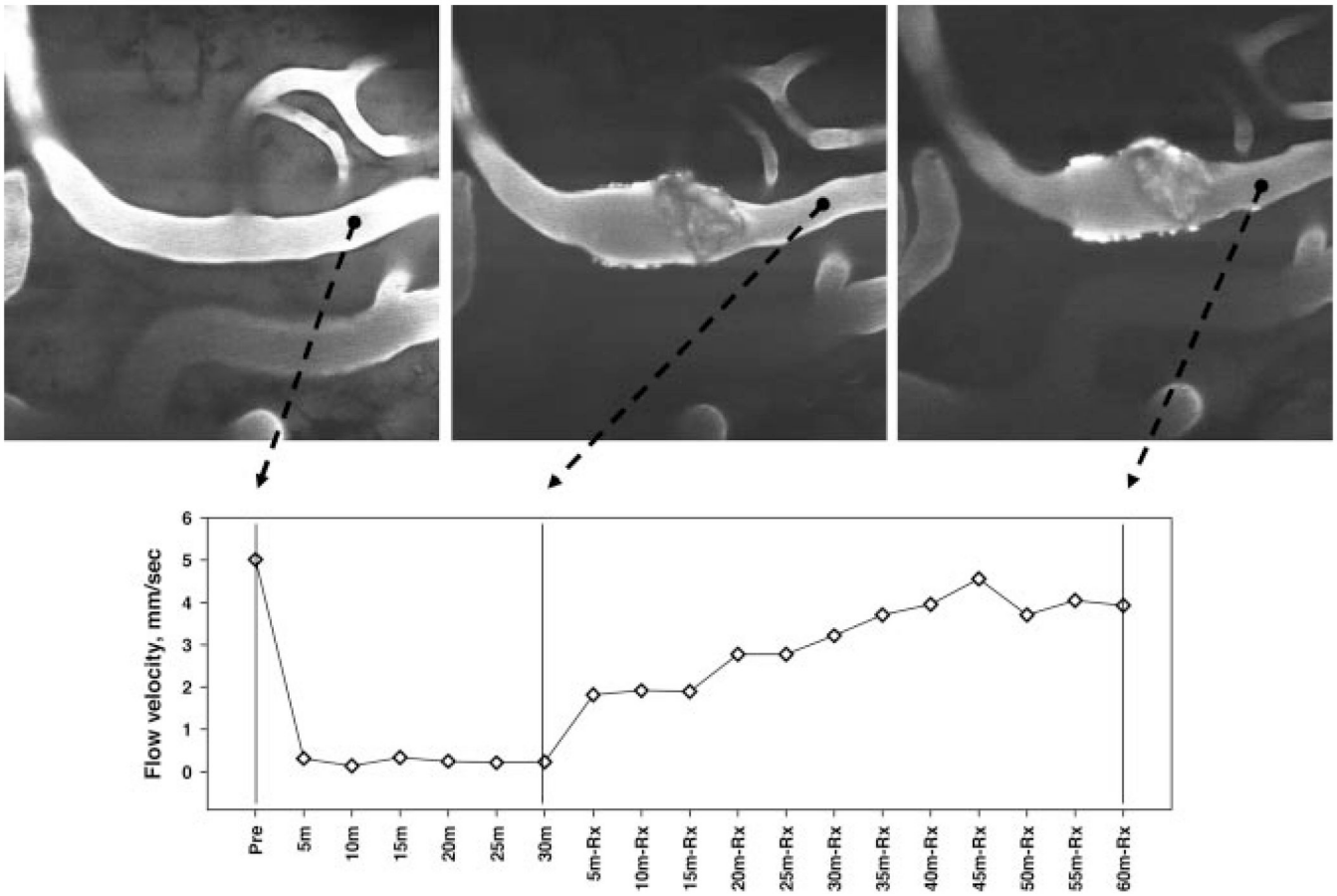

Figure 6.

Upper panels: cortical arteriole visualized with FITC-dextran at baseline (left), at 30 minutes after laser-induced thrombosis (middle), and at 90 minutes after ALB treatment (right). Lower panel presents microvascular flow velocities measured by line-scanning at 5-minute intervals. ALB therapy resulted in a prompt, progressive improvement in microvascular perfusion velocity distal to the arteriolar thrombosis. (20x objective).

Table

Physiological Variables

	Group	Baseline	30 Min Post-Thrombosis	End of Post-Rx Period
MAP, mm Hg	Albumin	108 ± 16	91 ± 7	83 ± 13
	Saline	103 ± 10	93 ± 12	80 ± 0
PO_2, mmHg	Albumin	113 ± 19	124 ± 20	124 ± 36
	Saline	117 ± 33	113 ± 36	128 ± 32
PCO_2, mmHg	Albumin	39.0 ± 4.9	39.4 ± 6.9	38.2 ± 4.4
	Saline	36.1 ± 3.9	37.5 ± 2.0	34.5 ± 1.4
pH, units	Albumin	7.45 ± 0.04	7.42 ± 0.04	7.45 ± 0.04
	Saline	7.48 ± 0.08	7.46 ± 0.06	7.49 ± 0.04
Glucose, mg/dL	Albumin	177 ± 47	190 ± 26	142 ± 48
	Saline	158 ± 37	167 ± 6	195 ± 49
Rectal temperature, °C	Albumin	36.3 ± 0.2	36.5 ± 0.3	36.5 ± 0.2
	Saline	36.2 ± 0.3	36.5 ± 0.2	36.6 ± 0.4

MAP indicates mean arterial pressure.
Values are mean + SD